

Proposal of highly sensitive optofluidic sensors based on dispersive photonic crystal waveguides

Sanshui Xiao and Niels Asger Mortensen

MIC – Department of Micro and Nanotechnology, NanoDTU,
Technical University of Denmark, DK-2800 Kongens Lyngby, Denmark.

E-mail: sanshui.xiao@mic.dtu.dk

Abstract. Optofluidic sensors based on highly dispersive two-dimensional photonic crystal waveguides are theoretically studied. Results show that these structures are strongly sensitive to the refractive index of the infiltrated liquid(n_l), which is used to tune dispersion of the photonic crystal waveguide. Waveguide mode-gap edge shifts about 1.2 nm for $\delta n_l=0.002$. The shifts can be explained well by band structure theory combined with first-order perturbation theory. These devices are potentially interesting for chemical sensing applications.

PACS numbers: 07.07.Df, 42.79.Gn, 42.70.Qs

Keywords: Sensors, Optical waveguide, Photonic Crystal

Submitted to: *J. Opt. A: Pure Appl. Opt.* , *Nanometa 2007 special issue*.

1. Introduction

Optofluidics, the marriage of nano-photonics and micro-fluidics, refers to a class of optical systems that integrate optical and fluidic devices [1]. Due to unique properties of fluids, such integration provides a new way for dynamic manipulation of optical properties and shows many potential applications [2, 3, 4, 5, 6, 7, 8, 9]. One of the most exciting optofluidic applications is to realize sensors, which can be used to detect, manipulate and sort cells, virus and biomolecules in fluidics. Many optical sensors operate by measuring the change in refractive index at the surface of the sensor with the method of e.g. surface-plasmon resonance, colorimetric resonances, interferometry in porous silicon. However, these methods require large-area beams and relatively large sensing area. Recently, Chow *et al.* demonstrated an ultra compact sensor employing a two-dimensional photonic crystal microcavity [10].

Photonic crystals (PhCs) are attractive optical materials for controlling and manipulating the flow of light [11, 12, 13]. Because of the unique light-confinement mechanism provided by the photonic bandgap, they have attracted much attention recently. It has been shown that they have many potential applications in optoelectronics, such as high-quality-factor filters [14], low-threshold lasers [15], optical switches, etc. In particular, PhCs are interesting for optofluidics since they naturally have voids where fluids can be injected [16, 17]. If we introduce a defect in a perfect PhC, optical properties of the defect can be easily reconfigured by selectively filling specific voids with liquid. PhC-based waveguides are highly dispersive, which has been used to slow down the propagation velocity of light [18]. In this paper, we will propose simple sensor structures based on highly dispersive photonic crystal waveguides. These structures are strongly sensitive to the refractive index of the liquid which is used to tune dispersion of the PhC waveguide. In the following we consider two different realizations of such a sensor.

2. Sensor structures and discussion

Let us first consider a photonic crystal waveguide shown in the inset of Fig. 1(a). The PhC studied in this paper is a two-dimensional PhC with a triangular array of air holes in an InP/GaInAsP dielectric background. We assume that the dielectric medium is non-absorbing, and has a constant index of refraction $n=3.24$. The radius of the air holes is $r=0.37a$, where a is the lattice constant. We calculate the photonic band structure by a plane-wave method [19] and the results show that the PhC possesses a wide photonic bandgap for TE polarization (magnetic field parallel to the air holes) for the normalized frequency a/λ between 0.2450 and 0.3744. A simple way of making a photonic crystal waveguide is to remove air holes within a single row. However, in our case we need to realize a non-solid waveguide serving also as a microfluidic channel or cavity. The PhC waveguide is formed by slightly lowering the radius of the air holes in a single row and these holes are used for local refractive index modulation

by selectively filling them with liquid. Presently, the common techniques for local index modulation are based on relatively weak nonlinearities, where $\delta n/n$ is of the order of 10^{-3} or lower. Other techniques are able to offer much higher $\delta n/n$, such as mechanical deformation, thermo-optics, and liquid crystal infusion. However, the effects tend to be of non-local nature. Nanofluidics provides both localized control and high refractive index modulation, which has attracted much attention. Recently, Erickson *et al.* experimentally demonstrated nanofluidic tuning of photonic crystal circuits [3]. Here, we will focus our study on transmission spectra of the PhC waveguide, shown in the inset of Fig. 1(a), for the waveguide with air holes being filled with different liquids. Transmission spectra for the PhC waveguide are obtained using the finite-difference

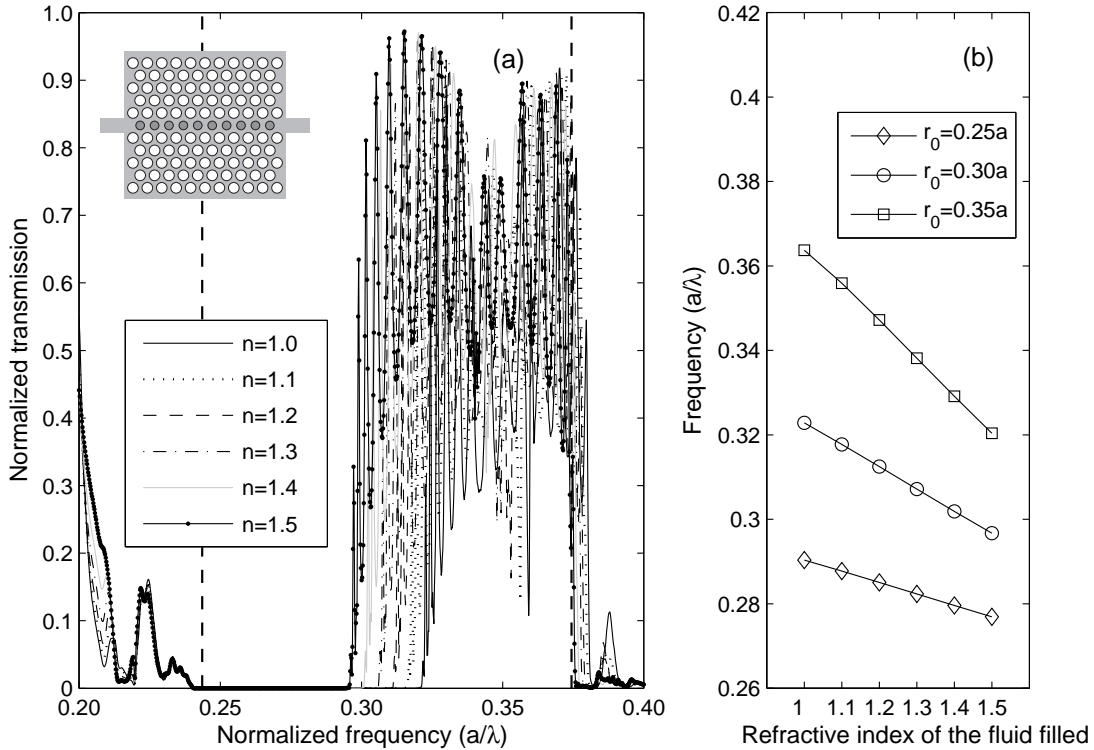


Figure 1. (a) Transmission spectra for the PhC waveguide, see inset, with the central air holes ($r_0=0.30a$) being filled by different liquids with refractive indices varying from $n_l=1.0$ to 1.5 in steps of $\delta n_l=0.1$. The two vertical dashed lines illustrate the band-gap region for the complete PhC. (b) Mode-gap edge as a function of the refractive index for the filled liquid.

time-domain (FDTD) method [20] with the boundaries treated within the framework of perfectly matched layers [21]. The in and out-coupling of light is facilitated by index-guiding slab waveguides with a TE-polarized fundamental mode as the source incident into the PhC waveguide. The width of the input/output waveguide is a and the refractive index is equivalent to that of the background of the PhC. It should be noted that the PhC waveguide may be multimode, in which case only modes with a

symmetry corresponding to the source can be excited. Figure 1(a) shows transmission spectra for the PhC waveguide with central air holes being filled by different liquids with the refractive index increasing from $n_l=1.0$ to $n_l=1.5$ in steps of $\delta n_l=0.1$, where the radius of the central air holes is $0.30a$. The bandgap edge of the complete PhC is indicated by two vertical dashed lines in Fig. 1(a). From Fig. 1(a), one knows that light, with a frequency in the bandgap, can propagate down the waveguide, and that there exists a mode-gap region in the lower frequency region, where propagation is inhibited. Although the PhC waveguide is a lossless one, the transmission is never close to unity due to the coupling loss at the two boundaries to the slab waveguides. Peaks in the transmissions arise from the Fabry–Perot oscillations from the two boundaries.

For the present application we are not interested in the details of the Fabry–Perot pattern in Fig. 1(a), but rather the spectral position of the mode-gap edge. As seen, the low-frequency mode-gap edge does not change with the refractive index of the liquid since it is a property of surrounding PhC. The positions for the low-frequency mode-gap edge are in agreement with that for band-gap edge indicated by the left vertical dashed line in Fig. 1(a). However, the high-frequency mode-gap edge is strongly dependent on the refractive index of the liquid, as shown in Fig. 1(b) for the cases of $r_0=0.25a$, $0.30a$ and $0.35a$. As an example, for the case of $r_0=0.30a$, the mode-gap edge changes from $a/\lambda=0.322869$ to 0.317751 when the air holes (with index $n_l=1$) are filled by a liquid of index $n_l=1.1$. From Fig. 1(b), one finds that the sensitivity becomes better as the hole size of the central increases from $r_0=0.25a$ to $0.35a$. However, calculated results show that the sensitivity does not depend much on the length of the device when the length is larger than $7a$. Now consider a commercial silicone fluid with a calibrated refractive-index accuracy of $\delta n_l=0.002$, as mentioned in Ref. [10], where the refractive index of the liquid varies from $n_l=1.446$ to 1.454 in increments of 0.002 . For the working wavelength around $1.55\mu\text{m}$ (here we choose $a=450\mu\text{m}$), the mode-gap edge shifts up to 0.5 nm for $\delta n_l=0.002$ when $r_0=0.30a$. For comparison, we note that the shift in resonant wavelength for the high-quality-factor (Q) PhC cavity is about 0.38 nm for $\delta n_l=0.002$ with a discrepancy of 4% between the calculated and experiment results [10]. The above results demonstrate that even such a simple PhC waveguide has potential applications as a sensitive sensor. Shifts in the frequency can be approximately analyzed by first-order electromagnetic perturbation theory yielding

$$\frac{\delta\lambda}{\delta n_l} \approx \frac{\lambda}{n_l} f, \quad (1)$$

where n_l is the refractive index of the liquid, λ is the working wavelength and f is the filling factor of the energy residing in the liquid, defined by

$$f = \frac{\int_l d\vec{r} \vec{E}(\vec{r}) \cdot \vec{D}(\vec{r})}{\int d\vec{r} \vec{E}(\vec{r}) \cdot \vec{D}(\vec{r})} \quad (2)$$

where $D = \epsilon E$ is the displacement field. The integral in the numerator of the filling factor f is restricted to the region containing the fluid while the other integral is over all space. For the low-frequency gap-edge mode mentioned above, $\delta\omega$ is nearly zero since

f is close to zero due to the bulk slab mode. f is about 20% for the high-frequency gap-edge mode when $n_l=1.446$. Thus, the problem is really that of maximizing the filling factor.

To further understand the physics behind it, we next support the picture by dispersion calculation for the PhC waveguide. For this purpose we use a plane-wave method [19]. The dispersion of the PhC waveguide in absence or presence of a fluid is shown in Fig. 2, which clearly illustrates how a waveguide mode forms within the bandgap region. Figure 2 (a)-(f) summarize the dispersions for the PhC waveguide, where the air holes, of radius $0.3a$, are filled by a liquid with a varying refractive index. The shaded regions are the projected band structure for TE slab modes, while the dots and circles represent the odd and even waveguide modes, respectively. The existence of a waveguide-mode gap is indicated by two horizontal dashed lines, where the mode-gap edges are in agreement with those obtained from the transmission spectra in Fig. 1(a). When increasing the refractive index of the liquid [going from panel (a) toward panel (f)], the high-frequency mode-gap edge (blue-dashed line) is significantly downward shifted. However, the low-frequency mode-gap edge, related to the band-gap edge, does not change as the refractive index of the liquid increases. We emphasize that all results obtained from band structures are consistent with those from the transmission spectra. The sensitivity of this structure is mainly attributed to the dispersion of the even waveguide mode denoted by circles in Fig. 2.

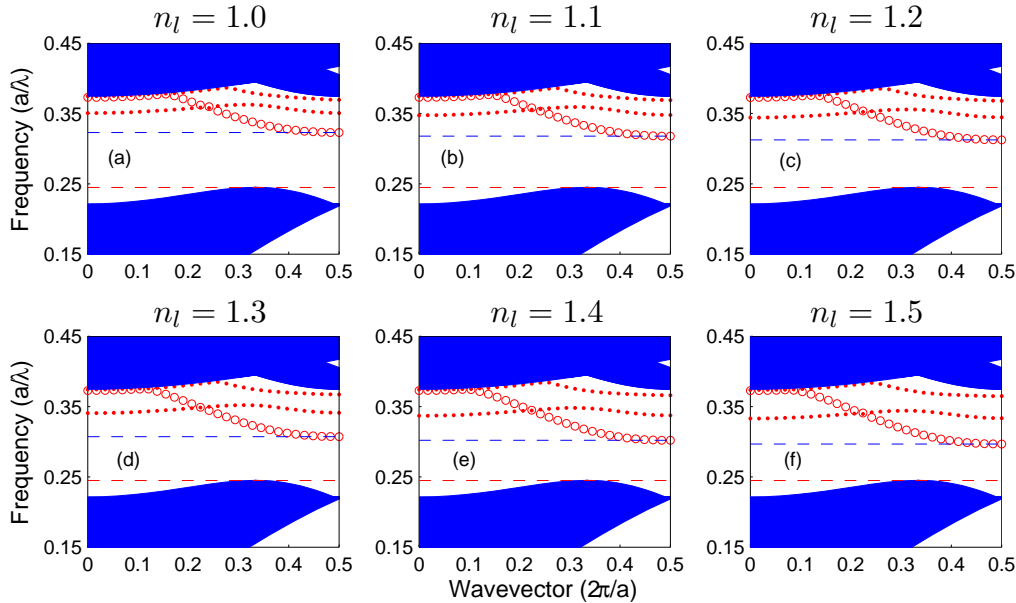


Figure 2. (Color on line) Dispersion of the PhC air-holes waveguide shown in the inset of Fig. 1(a), where the central air holes ($r_0=0.30a$) are filled by liquids with the refractive indices varying in steps of $\delta n_l = 0.1$. The circles and dots represent the even and odd waveguide mode, respectively.

Let us next consider another photonic crystal waveguide shown in the inset of

Fig. 3(a), where the waveguide is introduced by removing the background medium leaving us with an air channel waveguide. The width of the air channel waveguide is denoted by w , while other parameters and the input/output waveguide are totally same as those mentioned above. Transmission spectra, for the filled liquid with five different indices from $n_l=1.0$ to $n_l=1.4$ in increments of $\delta n_l=0.1$, are shown in Fig. 3(a) when $w=0.6a$. The band-gap region is also indicated by two vertical dashed lines. Similar to the result for the structure shown in Fig. 1(a), the waveguide mode-gap region still exists. The high-frequency mode-gap edge slightly changes as the refractive index of the liquid increases, while the low-frequency mode-gap edge is strongly dependant on the liquid. The low-frequency mode-gap edge is downward shifted as the refractive of the liquid increases. Here, we are only interested with the change of the position for the slow-frequency mode-gap edge, as shown in Fig. 3(b). One finds that the slope for the sensitivity hardly change when varying the width of the channel waveguide. Compared with the results for the high-frequency mode-gap edge shown in Fig. 1(b), from Fig. 3(b) one can find that such a waveguide shows a better sensitivity. From Fig. 3(b) one also find that sensitivity does not change much when varying the width of the channel waveguide from $w=0.4a$ to $0.6a$. The mode-gap edge shifts $\delta(a/\lambda)=0.0085$ when the air holes are filled by a liquid of index $n_l=1.1$ for the case of $w=0.6a$. For comparison we have $\delta(a/\lambda) = 0.0051$ for the structure shown in the inset of Fig. 1(a) when $r_0=0.30a$. The filling factor of the low-frequency gap-edge mode is about 44%, which is higher than that of the high-frequency gap-edge mode for the first structure shown in the inset of Fig. 1. Results from the numerical calculations are consistent with those obtained from the perturbation theory, Eq.(1). Again we consider a commercial silicone fluid with a calibrated refractive-index accuracy of $\delta n_l=0.002$. For the working wavelength around $1.55\mu\text{m}$ ($a=450\text{ nm}$), the mode-gap edge shifts up to 1.0 nm for $\delta n_l=0.002$. The proposed sensor relies strongly on the dispersion of the PhC waveguide mode and the presence of a mode gap. To further improve the sensitivity, we optimize the PhC waveguide structure by varying the radius (r_1) of the first row of air holes surrounding the channel waveguide. For simplicity we fix the width of the channel waveguide to $0.6 a$. We note that the device only works when the mode-gap exists and that the mode-gap will disappear as r_1 increases. By a careful design of the structure shown in the inset of Fig. 3(a), we have been able to improve the design further. For the working wavelength around $1.55\mu\text{m}$ ($a=450\text{ nm}$), the mode-gap edge shifts about 1.2 nm for $\delta n_l = 0.002$, when r_1 is tuned to $0.45 a$. Besides, this device has only a size about $5\mu\text{m} \times 5\mu\text{m}$, which is sufficiently compact for most applications. However, from Eq.(1), one knows that the sensitivity is proportional to the filling factor f for a specific working wavelength. Since the filling factor may be close to unity, photonic crystal devices may potentially have a sensitivity close to the limit.

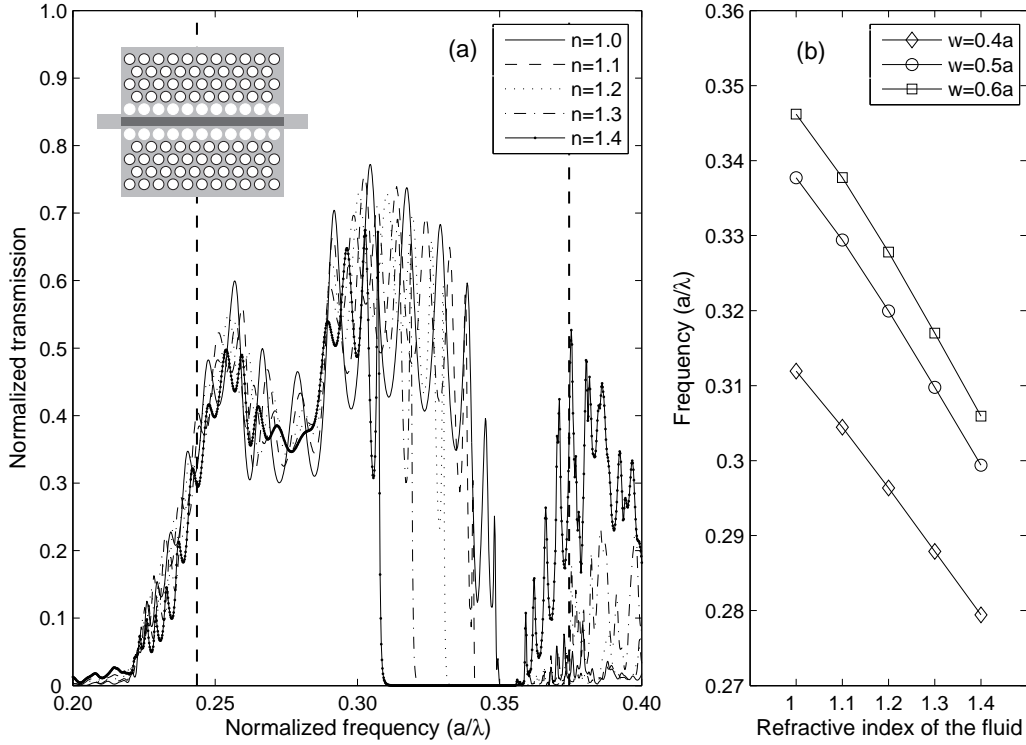


Figure 3. (a) Transmission spectra for the PhC channel waveguide ($w=0.60a$), see inset, being filled by different liquids. (b) Low-frequency mode-gap edge as a function of the refractive index for the filled liquid.

3. Summary

In this paper, we have theoretically studied optofluidic sensors based on highly dispersive two-dimensional photonic crystal waveguides. Our study shows that these structures are strongly sensitive to the refractive index of the liquid, which is used to tune dispersion of photonic crystal waveguides. For the working wavelength around $1.55\mu\text{m}$, waveguide mode-gap edge shifts up to 1.2 nm in increments of $\delta n_l = 0.002$. Compared with the air-holes waveguide, the channel waveguide in the PhC shows a better sensitivity, which can be explained by the first-order perturbation theory. Our study shown above is based on two-dimensional photonic crystal waveguides, while, it can be easily extended to a two-dimensional photonic crystal slab. Even though it may be difficult to inject liquid into the waveguides, we would like to emphasize that recently Erickson *et al.* experimentally demonstrated nanofluidic tuning in a similar structure [3]. These devices show a potential for chemical sensing applications.

Acknowledgments

This work is financially supported by the *Danish Council for Strategic Research* through the *Strategic Program for Young Researchers* (grant no: 2117-05-0037).

References

- [1] D. Psaltis, S. R. Quake, and C. H. Yang. Developing optofluidic technology through the fusion of microfluidics and optics. 2006 *Nature* 442 381–6
- [2] P. Domachuk, H. C. Nguyen, B. J. Eggleton, M. Straub, and M. Gu. Microfluidic tunable photonic band-gap device. 2004 *Appl. Phys. Lett.* 84 1838–40
- [3] D. Erickson, T. Rockwood, T. Emery, A. Scherer, and D. Psaltis. Nanofluidic tuning of photonic crystal circuits. 2006 *Opt. Lett.* 31 59–61
- [4] J. C. Galas, J. Torres, M. Belotti, Q. Kou, and Y. Chen. Microfluidic tunable dye laser with integrated mixer and ring resonator. 2005 *Appl. Phys. Lett.* 86 264101
- [5] C. Grillet, P. Domachuk, V. Ta’eed, E. Magi, J. A. Bolger, B. J. Eggleton, L. E. Rodd, and J. Cooper-White. 2004 Compact tunable microfluidic interferometer. *Opt. Express* 12 5440–47
- [6] H. Kurt and D. S. Citrin. Coupled-resonator optical waveguides for biochemical sensing of nanoliter volumes of analyte in the terahertz region. 2005 *Appl. Phys. Lett.* 87 241119
- [7] M. Gersborg-Hansen, S. Balslev, N. A. Mortensen, and A. Kristensen. A coupled cavity microfluidic dye ring laser. 2005 *Microelectron. Eng.* 78-79 185–89
- [8] Z. Y. Li, Z. Y. Zhang, T. Emery, A. Scherer, and D. Psaltis. Single mode optofluidic distributed feedback dye laser. 2006 *Opt. Express* 14 696–701
- [9] M. Gersborg-Hansen and A. Kristensen. Optofluidic third order distributed feedback dye laser. 2006 *Appl. Phys. Lett.* 89 103518
- [10] E. Chow, A. Grot, L. W. Mirkarimi, M. Sigalas, and G. Girolami. Ultracompact biochemical sensor built with two-dimensional photonic crystal microcavity. 2004 *Opt. Lett.* 29 1093–1095
- [11] S. John. Strong localization of photons in certain disordered dielectric superlattices. 1987 *Phys. Rev. Lett.* 58 2486–89
- [12] E. Yablonovitch. Inhibited spontaneous emission in solid state physics and electronics. 1987 *Phys. Rev. Lett.* 58 2059–62
- [13] J. D. Joannopoulos, R. D. Meade, and J. N. Winn. 1995 *Photonic crystals: molding the flow of light*. Princeton University Press, Princeton.
- [14] S. Xiao and M. Qiu. Surface-mode microcavity. 2005 *Appl. Phys. Lett.* 87 111102
- [15] H. G. Park, S. H. Kim, S. H. Kwon, Y. G. Ju, J. Y. Yang, J. H. Baek, S. B. Kim, and Y. H. Lee. Electrically driven single-cell photonic crystal laser. 2004 *Science* 305 1444–47
- [16] S. Xiao and N. A. Mortensen. Highly dispersive photonic band-gap-edge optofluidic biosensors. 2006 *J. Eur. Opt. Soc., Rapid Publ.* 1 06026
- [17] N. A. Mortensen and S. Xiao. Liquid-infiltrated photonic crystals: Ohmic dissipation and broadening of modes. 2006 *J. Eur. Opt. Soc., Rapid Publ.* 1 06032
- [18] H. Gersen, T. J. Karle, R. J. P. Engelen, W. Bogaerts, J. P. Korterik, N. F. van Hulst, T. F. Krauss, and L. Kuipers. Real-space observation of ultraslow light in photonic crystal waveguides. 2005 *Phys. Rev. Lett.* 94 073903
- [19] S. G. Johnson and J. D. Joannopoulos. Block-iterative frequency-domain methods for Maxwell’s equations in a planewave basis. 2001 *Opt. Express* 8 173–90
- [20] A. Taflov. 2000 *Computational Electrodynamics: The Finite-Difference Time-Domain Method*. Artech House INC, Norwood, 2 edition.
- [21] J. P. Berenger. A perfectly matched layer for the absorption of electromagnetic waves. 1994 *J. Comput. Phys.* 114 185–200